Effects of Fe^{3+} and Ag^+ on Column Bioleaching of a Low-grade Sulfide Copper Ore

Liangyou Jiang[1], Dezhou Wei[1,], Wengang Liu[1,2], Kaikai Liu[1] and Hao Zhang[1,*]*

[1] School of Resources and Civil Engineering, Northeastern University, Shenyang 110819, China;
[2] State Key Laboratory of Mineral Processing, Beijing General Research Institute of Mining and Metallurgy, Beijing 100160, China;
[*]E-mail: dzwei@mail.neu.edu.cn (Dezhou Wei); zhanghaoe66@163.com (Hao Zhang)

Due to the consumption of high-grade ores and the increasing demand for copper, the utilization of low-grade copper-bearing ores has become a prominent area of research. In this study, column bioleaching was adopted to separate low-grade copper ore. The effects of Fe^{3+} and Ag^+ on the electrochemical characteristics and column bioleaching of the ore were investigated. The bioleaching ratio and bioleaching rate, as well as the changes to the pH and the redox potential under the effect of Fe^{3+} and Ag^+ were explored. The morphology and phase differences of the leaching residues were compared by XRD patterns and SEM-EDS images, respectively. The results showed Fe^{3+} could enhance the bioleaching of the ore at an optimal concentration of 0.06 mol·L^{-1}. The Fe^{3+} concentration of the leaching solution in bioleaching with Ag^+ was higher than that without Ag^+. Ag^+ could improve both the bioleaching ratio and the bioleaching rate of the Cu^{2+}. Leaching residues with rougher surfaces could be obtained with Ag^+. Fe^{3+} was one of the important elements for the redox action in leaching solution. The enhanced extraction of Cu in the presence of Fe^{3+} caused the formation of minerals with high iron content.
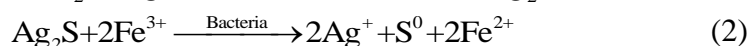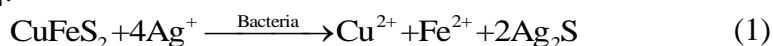
1. INTRODUCTION

As one of the essential metal resources, copper plays an indispensable role in the national economy and in peoples' livelihoods. The broad applications of copper, such as in electric vehicles, results in high consumption [1]. As a result, the utilization of low-grade ores are of increasing concern [2,3]. However, traditional techniques, including pyrometallurgy and chemical treatment, cannot be used to commercially process these kinds of ores [4].

Bioleaching is one of the effective ways to extract valuable minerals from solid wastes, complex polymetallic ores, and low-grade ores [5-7]. Additionally, it has been used to successfully treat low-grade copper ores. Chalcopyrite is an important copper resources. The bioleaching of high-grade chalcopyrite, including the bioleaching mechanisms and the influence of metal ions, has been widely researched. [10-13][1,7,14]. However, the leaching efficiency of the chalcopyrite can be severely deteriorated by the passive film formed during the bioleaching [8,9]. The problems of long a leaching cycle and a low leaching rate are still unsolved. Therefore, it is essential to explore feasible solutions to enhance the bioleaching efficiency of the chalcopyrite to broaden applications of bioleaching and enhance the utilization of the low-grade ores.

Metal ions, such as Ag^+ and Hg^{2+}, have been researched to accelerate the bioleaching of minerals. Ag^+ was verified to play a significant catalytic role in improving the leaching efficiency [15-17]. The catalytic mechanism was described as the rapid reactions between Ag^+ and chalcopyrite, which are shown as follows [18-20]:

$$CuFeS_2 + 4Ag^+ \xrightarrow{\text{Bacteria}} Cu^{2+} + Fe^{2+} + 2Ag_2S \qquad (1)$$

$$Ag_2S + 2Fe^{3+} \xrightarrow{\text{Bacteria}} 2Ag^+ + S^0 + 2Fe^{2+} \qquad (2)$$

As seen from the above reactions, the iron ions play vital roles in both the catalytic reaction and the bioleaching. Further studies verified that the oxidization of Fe^{2+} into Fe^{3+} can accelerate the bioleaching of chalcopyrite [21, 22]. Moreover, the effects of iron ions on the dissolution kinetics of the chalcopyrite, as well as the solution redox potentials, were explored to clarify the specific roles the iron ions played [23-28]. Although the individual effects of Ag^+ and iron ions on chalcopyrite bioleaching have been investigated, the combined influences of the ions on the low-grade copper ores are rarely reported.

In this work, the bioleaching of a low-grade copper ore was catalyzed by Ag^+. The effects of different initial concentrations of Fe^{3+} on the bioleaching were researched, and the effects of the Ag^+ on bioleaching and Fe^{3+} were also investigated. Measurements including X-ray diffraction (XRD), Scanning Electron Microscopy (SEM) and Energy Dispersive X-ray Spectroscopy (EDS) were used to investigate the bioleaching residues.

2. EXPERIMENTAL

2.1. Mineral Samples

The low-grade copper ore samples were obtained from Jiama in Tibet Province of China. The ore was first crushed to −10 mm by a jaw crusher (PEF100×60 mm). In addition, a small part of the crushed ore was subsampled and finely ground for chemical analysis. As shown in Table 1, the copper content of the low-grade ore was approximately 0.26%. SiO_2 was the main gangue mineral and its content was as high as 68.05%. The main minerals of the ore samples are chalcopyrite, zigueline, langite, and malachite, which are verified by the X-ray diffraction (XRD) patterns.

All the reagents used in this work were purchased from China National Pharmaceutical with analytical pure.

Table 1. Main chemical composition analysis of the ore sample

Composition	Cu	Fe	S	SiO_2	CaO	MgO	Al_2O_3
Content (%)	0.26	3.54	3.58	68.05	1.14	1.0828	13.61
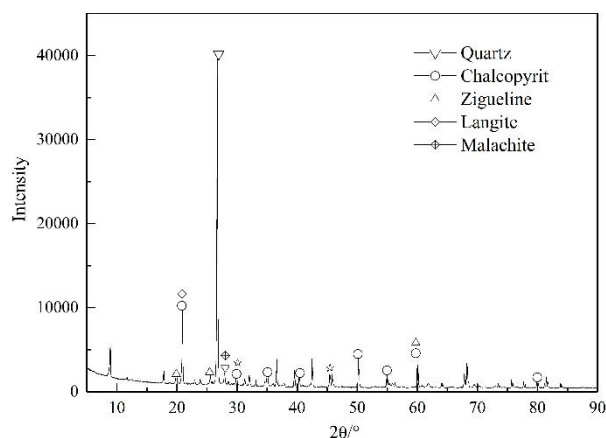
Figure 1. XRD pattern of the low- grade copper ore sample

2.2. Microorganism and culture media

The bacteria *Acidithiobacillus ferrooxidans* (*At. ferrooxidans*), which were collected from the acid mine waters of Jiama in Tibet Province of China, was used for the bioleaching of the ore. The microorganisms were cultured in a 9K medium, which consisted of basic salt solutions (containing 3.0 $g \cdot L^{-1}$ $(NH_4)_2SO_4$, 0.1 $g \cdot L^{-1}$ KCl, 0.5 $g \cdot L^{-1}$ K_2HPO_4, 0.5 $g \cdot L^{-1}$ $MgSO_4 \cdot 7H_2O$, and 0.01 $g \cdot L^{-1}$ $Ca(NO_3)_2$) and 44.2 $g \cdot L^{-1}$ $FeSO_4 \cdot 7H_2O$ as the energy sources. The pH value of the basic salt solution was kept at 1.6 and sterilized at 0.1 MPa and 120°C.

The leaching ratio *X* and the leaching rate *v* were important indexes for evaluating the bioleaching and were calculated as follows:

$$X=VC \times 100\%/mw \qquad (3)$$
$$v= (C_1-C_0)/(t_1-t_0) \qquad (4)$$

where *V* was the volume of leaching solution, L. *C* was the concentration of Cu^{2+} in the leaching solution, $g \cdot L^{-1}$. *m* was the weight of the ore, g. *w* was the Cu content of the pristine ore, %. t_0, t_1 were the adjacent sampling time, d. Lastly, C_0, C_1 were the Cu^{2+} concentrations corresponding to the different sampling times of t_0 and t_1, respectively, $g \cdot L^{-1}$.

2.3. Column bioleaching

A perspex column was used for the bioleaching of the low-grade copper ore. The 1 kg sample, was first loaded into the column. Then, 5 L of leaching solution containing a 10% volume ratio of bacteria was sprayed at the top of the samples. The leaching solution was collected at the bottom and

circulated to the top by a constant-flow pump at last. The schematic diagram of the column leaching is shown in Figure 2.
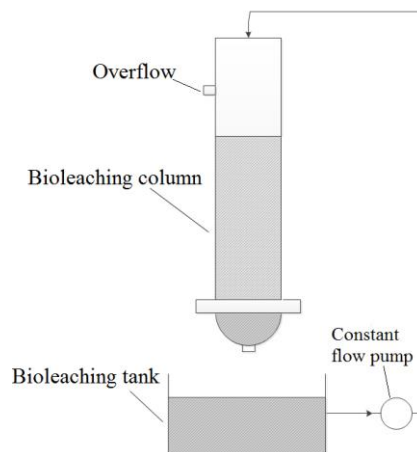

Figure 2. Schematic diagram of the bioleaching column

2.4. Characterization

The leaching solution was sampled periodically to measure the metal ion content. The concentration of the dissolved metal ions was analyzed by inductively coupled plasma-atomic emission spectrometry (ICP-AES) (America Leeman Co. PROFILE SPEC). The variations of redox potential and pH in were monitored by a digital pH meter (PB-10, Sartorius, Germany). The redox potential was measured against a reference platinum electrode (PY-ASI, Sartorius, Germany). All the tests were conducted at 25°C.

After bioleaching, the residues were cleaned by dilute acid solutions and dried in an oven under 60 °C. The dry residues were then crushed and ground to -0.074 mm for X-ray Diffraction (XRD) and Scanning Electron Microscope (SEM) analyses. Based on the XRD and SEM results, the changes in mineral composition and morphology were investigated.

3. RESULTS AND DISCUSSION

3.1. Effects of Fe^{3+} on column bioleaching of the low-grade copper ore

The oxidation of Fe^{2+} can provide energy for the growth and reproduction of *At. ferrooxidans*. Additionally, the oxidation products (Fe^{3+}) are the main oxidant for oxidizing copper-bearing sulfide minerals [29-32]. The bioleaching of the low-grade copper ore was controlled by the Fe^{3+} concentration in the solution. Therefore, it is essential to investigate the specific effects of the Fe^{3+} in order to improve the bioleaching efficiency.

3.1.1. Effects of initial Fe^{3+} concentration on pH of the leaching solution
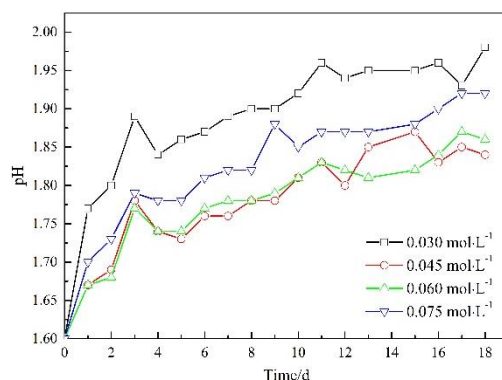

Figure 3. Leaching solution pH changes as a function of time for different initial Fe^{3+} concentrations

As the leaching solution pH is an important index that can influence both the growth of bacteria and the dissolution of minerals, the pH changes as a function of initial Fe^{3+} concentration was recorded during the bioleaching [33-35]. As seen from Figure 3, the pH increased as bioleaching progressed. Due to the reproduction of the microorganism, the significant peaks occurred on the 3rd day of bioleaching. The pH values of the leaching solution were the highest with an initial Fe^{3+} concentration of 0.03 mol·L^{-1}. The low Fe^{3+} concentration accelerated the oxidation of Fe^{2+}, which in turn accelerated the dissolution of the chalcopyrite [36]. The rate of increase of the pH became lower with a high initial Fe^{3+} concentration. When the solution with 0.06 mol·L^{-1} Fe^{3+} was used for the bioleaching, the pH was the lowest. However, for the high Fe^{3+} concentration of 0.075 mol·L^{-1}, the precipitation reaction of the Fe^{3+} caused the pH to increase.

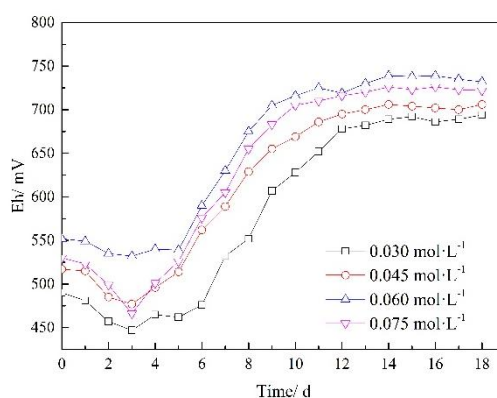*3.1.2. Effects of initial Fe^{3+} concentration on redox potential of the leaching solution*

Figure 4. Redox potential changes as a function of time for different initial Fe^{3+} concentrations

Fe^{2+} is the essential element and energy source for the growth of *At. ferrooxidans*, and Fe^{3+} can influence the chemical reactions and solid-liquid mass transfer in the leaching [37-39]. It is critical to

detect the ions' concentration changes. As the redox potential of the leaching solution could reflect the concentration ratio of Fe^{3+} and Fe^{2+} [40-41], the redox potential changes under different initial Fe^{3+} concentrations were recorded and plotted in Figure 4. The oxidation of Fe^{2+} increased the redox potential of the leaching solution. As a result, the redox potential of the leaching solution presented an overall upward trend as the bioleaching progressed. A small drop occurred on the 3rd day of the bioleaching, which was ascribed to the reproduction of the microorganism. With a lower Fe^{3+} concentration, the oxidation of Fe^{2+} was promoted. Then, the solution with an initial Fe^{3+} concentration of 0.03 $mol \cdot L^{-1}$ showed the lowest redox potential. Additionally, the redox potentials increased with an increasing Fe^{3+} concentration. However, as the excessive Fe^{3+} precipitated, the redox potential of the solution with the highest Fe^{3+} concentration of 0.075 $mol \cdot L^{-1}$ was lower than that of 0.06 $mol \cdot L^{-1}$.

3.1.2. *Effects of initial Fe^{3+} concentration on leaching ratio and leaching rate*

The changes in the leaching ratio and the leaching rate as a function of the initial Fe^{3+} concentration are displayed in Figure 5. As shown in Figure 5a, the leaching ratio first increased and then held stable after 14 days. As the initial Fe^{3+} concentration increased from 0.03 $mol \cdot L^{-1}$ to 0.06 $mol \cdot L^{-1}$, the leaching ratio increased. However, the leaching ratio decreased for the solution containing 0.075 $mol \cdot L^{-1}$ Fe^{3+}. The leaching ratio was the highest with 0.06 $mol \cdot L^{-1}$ Fe^{3+}, and it reached approximately 30% after 18 days. Therefore, the optimal initial Fe^{3+} concentration for bioleaching was set at 0.06 $mol \cdot L^{-1}$.
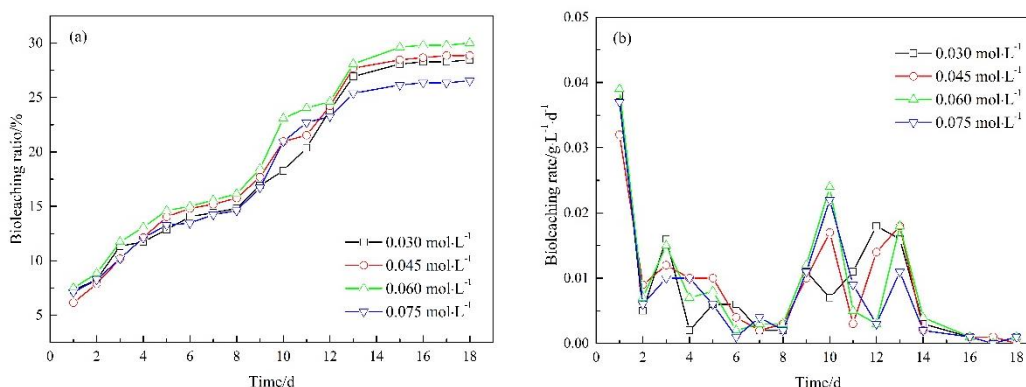

Figure 5. Changes in (a) leaching ratio and (b) leaching rate as a function of time for different initial Fe^{3+} concentrations

The changes in the leaching rate under different initial Fe^{3+} concentrations are shown in Figure 7b. As bioleaching continued, the leaching rate fluctuated. The bioleaching was the fastest on the 1st day. Further the rate of bioleaching decreased over the next 7 days due to the reproduction of the microorganism. For the higher initial Fe^{3+} concentrations of 0.045 $mol \cdot L^{-1}$, 0.06 $mol \cdot L^{-1}$ and 0.075 $mol \cdot L^{-1}$, the leaching rate showed two peaks on the 10th day and the 13th day. For the solution with 0.03 $mol \cdot L^{-1}$ Fe^{3+}, a single significant peak occurred on the 12th day. The plots changed, such as "M" from the 8th day to the 14th day, which reflected the exponential phase of microbial growth. During this period, Fe^{3+} was not hydrolyzed in large quantities, which was beneficial for the bioleaching.

3.2. Effects of Ag^+ on column bioleaching of the low-grade copper ore
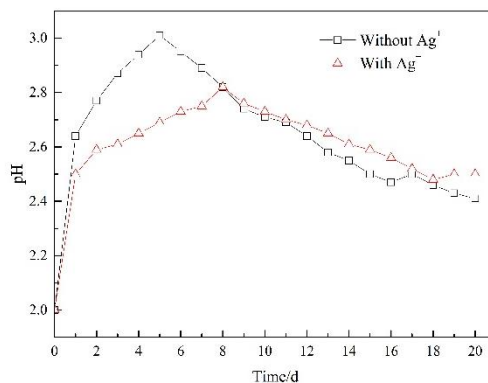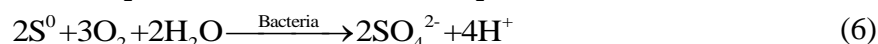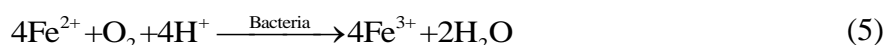
3.2.1. Effects of Ag^+ on pH of the leaching solution

Figure 6. Effects of Ag^+ on pH changes of the leaching solution (C_{Ag+}=10 mg·L^{-1})

Figure 6 shows the comparative pH changes of the leaching solution with or without Ag^+ (10 mg·L^{-1}). Due to the existence of alkaline gangue minerals, the acid-base neutralization reactions occurred and consumed portions of the acid. Therefore, the pH of the leaching solution increased at first. As the bioleaching reaction progressed, the S^{2-} was oxidized and transformed into sulfuric acid due to the catalysis of bacteria. Then, the pH of the leaching solution decreased. Without Ag^+, the pH increased from 2.0 to 3.0 within the first 6 days and then dropped to 2.4 slowly in the next 14 days. The pH changes presented a similar trend when Ag^+ was added. With Ag^+, the rate of increase of the pH decreased after the first 2 days. Additionally, the pH reached a peak at 2.8 on the 8th day. The pH plot when Ag^+ was present was flatter, indicating Ag^+ could moderate the pH changes in the leaching solution.

3.2.2. Effects of Ag^+ on redox potential of the leaching solution

The redox potential changes of the leaching solution with and without Ag^+ (10 mg·L^{-1}) are shown in Figure 7. In the first 3 days, both redox potentials with and without Ag^+ stayed unchanged at approximately 450 mV. Without Ag^+, the redox potential increased rapidly and reached 650 mV on the 8th day of the bioleaching. Equations (1) and (2) showed that, when Ag^+ was added, the oxidization of Ag_2S consumed Fe^{3+} and resulted in a lower redox potential. Meanwhile, as equations (5) and (6) show, the Fe^{2+} and S^0 were oxidized in the presence of bacteria [36].

$$4Fe^{2+}+O_2+4H^+ \xrightarrow{\text{Bacteria}} 4Fe^{3+}+2H_2O \qquad (5)$$
$$2S^0+3O_2+2H_2O \xrightarrow{\text{Bacteria}} 2SO_4^{2-}+4H^+ \qquad (6)$$

Therefore, in the bioleaching with Ag^+, the redox potential was lower than that without Ag^+. It could only reach a peak at 550 mV on the 8th day. Additionally, both of the redox potentials stayed stable after 8 days.
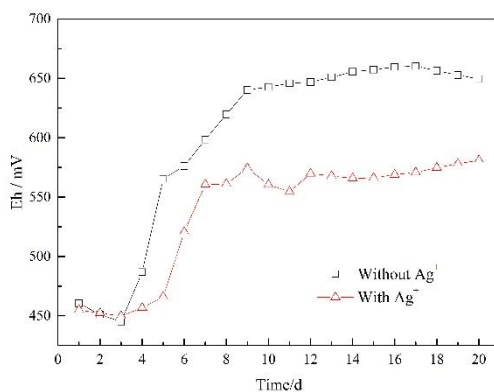
Figure 7. Effects of Ag^+ on redox potential changes of the leaching solution (C_{Ag+}=10 mg·L^{-1})

3.2.3. Effects of Ag⁺ on leaching ratio and leaching rate

Figure 8a shows the changes in the leaching ratio with and without Ag^+ (10 mg·L^{-1}). Both leaching ratios increased steadily over 20 days. Further, they reached peaks of 18.46% and 15.58% for bioleaching with and without Ag^+, respectively. As the bioleaching ratio under the influence of Ag^+ was higher than that without Ag^+, it could be deduced that Ag^+ had a remarkably positive effect on the bioleaching of the low-grade copper ore, especially between the 2nd day and the 9th day.

The leaching rate under the effect of Ag^+ is depicted in Figure 8b. The leaching rate was higher in the first three days for bioleaching both with and without Ag^+ and reached peaks on the 3rd day. Then, the leaching rate decreased rapidly on the 4th day and fluctuated during the remaining bioleaching days. The leaching rate with Ag^+ was higher than the rate without Ag^+. Obviously, Ag^+ could improve both the leaching ratio and leaching rate in the column bioleaching of low-grade copper ore.
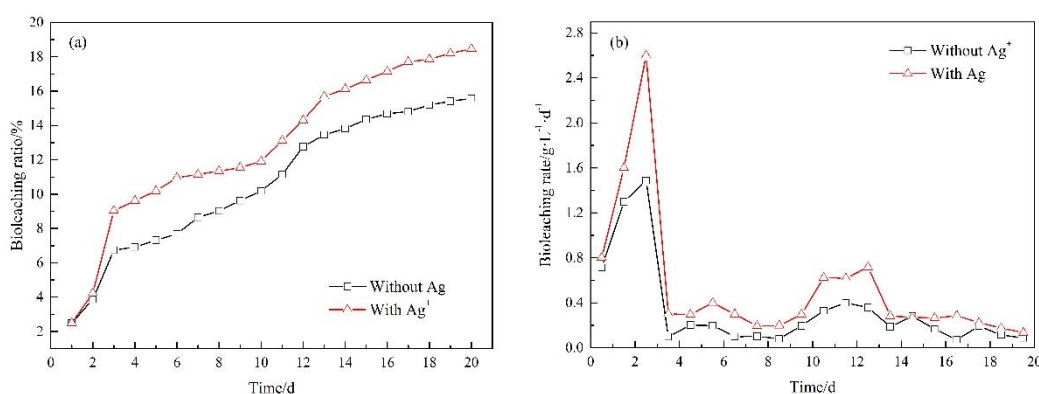

Figure 8. Effects of Ag^+ on (a) leaching ratio and (b) leaching rate (C_{Ag+}=10 mg·L^{-1})

3.2.4. Effects of Ag⁺ on Fe³⁺ concentration of the leaching solution

To further explore the comprehensive effects of Ag^+ on the bioleaching of low-grade copper ore, the concentration changes of the iron ions with and without Ag^+ were compared. The plots in Figure 8a and Figure 8b shows that, except for the first 6 days, the concentration of Fe^{3+} was higher with Ag^+ than

without Ag^+. Without Ag^+, the Fe^{3+} concentration reached peaks on the 2nd day, the 5th day and the 14th day. However, the peaks samples with Ag^+ were centered between the 8th day and the 17th day. The high concentration of the Fe^{3+} accelerated the oxidation and dissolution efficiency of the ore. As a result, both the leaching ratio and leaching rate were improved.
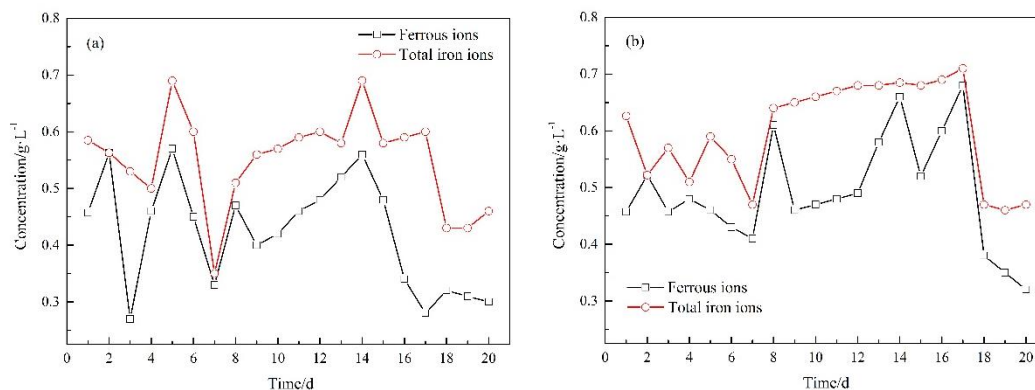

Figure 9. Iron ion concentration changes (a) without Ag^+ and (b) with Ag^+ (C_{Ag+}=10 mg·L^{-1})
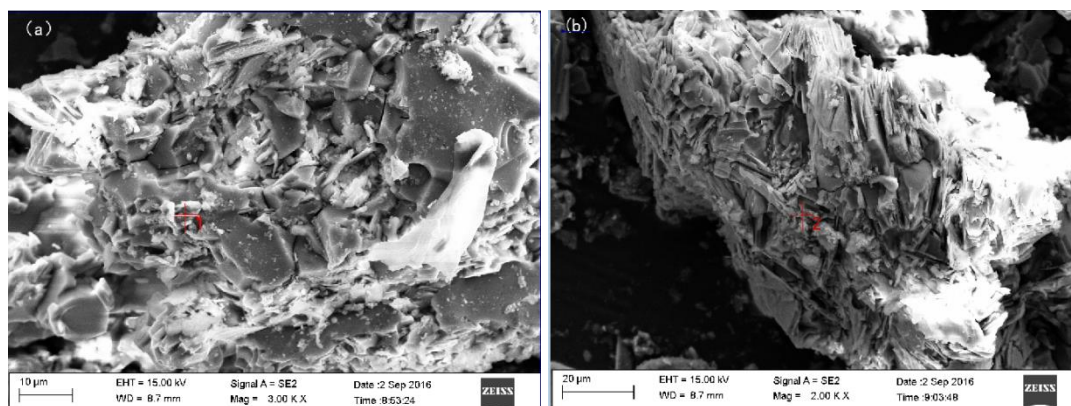
3.3. Analysis of the bioleaching residues

Figure 10. SEM images of leaching residues (a) without Fe^{3+} and (b) with Fe^{3+} ($C_{Fe^{3+}}$= 0.06 mol·L^{-1})

The differences in the morphology and phase of the bioleaching residues were compared by means of SEM-EDS and XRD. In Figure 10, irregular and poor porosity holes, which resulted from the surface reactions during the bioleaching, could be easily observed for both residues. Comparing the two images, the residue surface of the sample with Fe^{3+} was rougher than that of the sample without Fe^{3+}. Without Fe^{3+}, rough, round concave spots and shallow gullies were distributed on the surface. While with Fe^{3+}, a long and deep gully could be observed on the residue surface, indicating that the more effective and thorough bioleaching could be enhanced by Fe^{3+}. The accompanying EDS plots in Figure 11 shows that the main elements on the residue surface were sulfur, potassium, and iron. Comparing the EDS spectra of the two residues, the content of Si on the residue with Fe^{3+} was higher than that without Fe^{3+}, indicating more Cu was extracted from the ore.
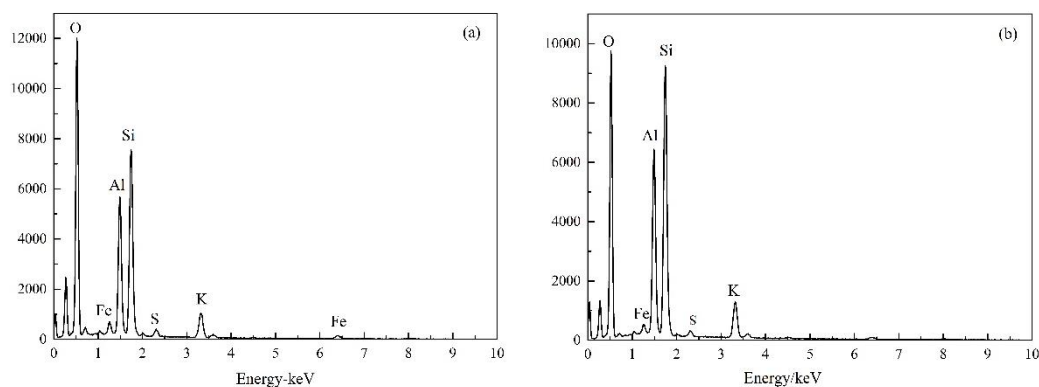
Figure 11. EDS spectrographs of leaching residues (a) without Fe^{3+} and (b) with Fe^{3+} ($C_{Fe^{3+}}= 0.06$ mol·L^{-1})

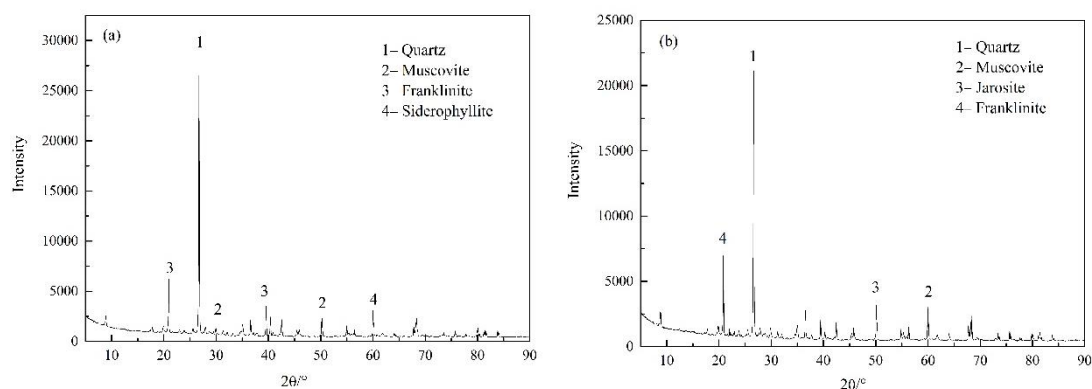**Figure 12.** XRD patterns of leaching residues (a) without Fe^{3+} and (b) with Fe^{3+} ($C_{Fe^{3+}}= 0.06$ mol·L^{-1})

The phase changes with and without Fe^{3+} were characterized by the XRD patterns of the bioleaching residues, which are shown in Figure 12. Quartz and Fe-bearing minerals, including muscovite and franklinite, were the main minerals of the residues. With the addition of Fe^{3+}, jarosite, which had a high iron content, could be detected, indicating that the Fe^{3+} enhanced the displacement of Cu. As a result, the bioleaching of the copper ore was enhanced.

4. CONCLUSIONS

In this study, column bioleaching was adopted to treat a low-grade copper ore. For effective separation of the ore, the effects of Fe^{3+} and Ag^+ on electrochemical characteristics and bioleaching of the ore were investigated. With a leaching solution containing 0.06 mol·L^{-1} Fe^{3+}, the leaching ratio could reach 30% in 20 days. Both Fe^{3+} and Ag^+ could enhance the bioleaching of the low-grade copper ore. Significant increases in the bioleaching ratio and bioleaching rate could be obtained by adding Ag^+. With Ag^+, the bioleaching ratio could reach 18.46% in 20 days, which is 2.88% higher than that without Ag^+. The redox reaction between Ag_2S and Fe^{3+} changed the concentration of Fe^{3+} and the redox potential of

the leaching solution. Moreover, when exploring the comprehensive effects of Fe^{3+} and Ag^+, the Fe^{3+} concentration of the leaching solution in the presence of Ag^+ was higher than that without Ag^+. Irregular and poor porosity holes could be observed on the residue surface. A rougher surface with a deep and long gully was obtained when Fe^{3+} was added. Based on the analysis of the SEM-EDS and XRD, the main minerals in the bioleaching residues were quartz and iron-bearing minerals. Due to the enhanced replacement reactions in the presence of Fe^{3+}, jarosite, a mineral with a high iron content, was generated.

References

1. L. Copper, *Metal Bulletin Daily*, 13 (2018) 211.
2. J.E. Tilton, G. Lagos, *Resour. Policy.*, 32 (2007) 19.
3. T. Norgate, S. Jahanshahi, *Miner. Eng.*, 23 (2010) 65.
4. H.M. Abdulla, H.S. Taher, H.A. Ibrahim, *Geomicrobiolo. J*, 35 (2018) 91.
5. H.R. Watling, *Hydrometallurgy*, 84 (2006) 81.
6. D.B. Johnson, *Curr. Opin. Biotech.*, 30 (2014) 24.
7. S. Yin, L. Wang, E. Kabwe, X. Chen, R. Yan, K. An, L. Zhang, A. Wu, *Minerals*, 8 (2018) 1.
8. C. Yang, F. Jiao,. W. Qin, *Minerals*, 8 (2018) 1.
9. S.F. Wu, C.R. Yang, W.Q. Qin, F. Jiao, J. Wang, Y.S. Zhang, *Trans. Nonferrous. Met. Soc. China*, 25 (2015) 4110.
10. Y.H. Hu, G.Z. Qiu, J. Wang, D.Z. Wang, *Hydrometallurgy*, 64 (2002) 81.
11. H. Abdollahi, M. Noaparast, S.Z. Shafaei, Z. Manafi, J. A. Muñoz, O.H. Tuovinen, *Int. Biodeter. Biodegr.*, 104 (2015) 194.
12. S. Deng, G.H. Gu, J. Ji, B. Xu, *Anal. Bioanal. Chem.*, 410 (2018) 1725.
13. Y. Yang, W. Liu, M. Chen, *Miner. Eng.*, 70 (2015) 99.
14. Z. Niu, Q. Huang, J. Wang, Y. Yang, B. Xin, S. Chen, *J. Hazard. Mater.* 298 (2015) 170.
15. A. Ballester, F. González, M.L. Blázquez, J.L. Mier, *Hydrometallurgy*, 23 (1990) 221.
16. A. Ballester, F. González, M.L. Blázquez, C. Gómez, J.L Mier, *Hydrometallurgy*, 29 (1992) 145.
17. K. Oyama, K. Shimada, J.I. Ishibashi, H. Miki, N. Okibe, *Hydrometallurgy*, 177 (2018) 197.
18. J.D. Miller, H.Q. Portillo, *13th International Mineral Processing Congress*, 13 (1981) 851.
19. L. Ahonen, O.H. Tuovinen, *Hydrometallurgy*, 24 (1990) 219.
20. L. Sukla, G. Chaudhury, R. Das, *T. I. Min. Metall. C*, 99 (1990) 43.
21. Y. Wang, Z. Song, N. Everaert, B. D. Ketelaere, H. Willemsen, E. Decuypere, J. Buyse, *Physi. Behav.*, 132 (2014) 66.
22. L. Ma, X. Wang, X. Feng, Y. Liang, Y. Xiao, X. Hao, H. Yin, H. Liu, X. Liu, *Bioresource Technol.*, 223 (2017) 121.
23. K.A. Third, R. Cord-Ruwisch, H.R. Watling, *Biotechnol. Bioeng.*, 78 (2002) 433.
24. N. Hiroyoshi, H. Miki, T. Hirajima, M. Tsunekawa, *Hydrometallurgy*, 57 (2000) 31.
25. K.A. Third, R. Cord-Ruwisch, Watling H.R., *Hydrometallurgy*, 57 (2000) 225.
26. N. Hiroyoshi, M. Hirota, T. Hirajima, M. Tsunekawa, *Hydrometallurgy*, 47 (1997) 37.
27. J. Vilcáez, C. Inoue, *Miner. Eng.*, 22 (2009) 951.
28. W.G. Liu, L. Zhao, W.B. Liu, T. Yang, H. Duan, *Miner. Eng.*, 134 (2019) 394.
29. Y. Zhou, X. Huang, G. Huang, X. Bai, Y. Li, *Chin. J. Biotechnol.*, 24 (2008) 1993.
30. R.L. Yu, J. Liu, A. Chen, D.L. Zhong, Q. Li, W.Q. Qin, G.Z. Qiu, G.H. Gu, *T. Nonferr. Metal. Soc.*,

23 (2013) 231.
31. H.C. Liu, J.L. Xia, Z.Y. Nie, *Hydrometallurgy*, 156 (2015) 40.
32. A.D. Dorado, M. Solé, C. Lao, P. Alfonso, X. Gamisans, *Miner. Eng.*, 39 (2012) 36.
33. H.C. Liu, J.L. Xia, Z.Y. Nie, C.Y. Ma, L. Zheng, *Miner. Eng.*, 98 (2016) 80.
34. R.L. Yu, J. Liu, J.X. Tan, W.M. Zeng, L.J. Shi, G.H. Gu, W.Q. Qin, G.Z. Qiu, *Int. J. Min. Met. Mater.*, 27 (2014) 311.
35. Z.J. Yu, R.L. Yu, A.J. Liu, J. Liu, W.M. Zeng, X.D. Liu, G.Z. Qiu, *T. Nonferr. Metal. Soc.*, 27 (2017) 406.
36. J. Ma, J.X. Wang, B. Wu, J.K. Wen, H. Shang, M.L. Wu, *Chin. J. Nonferr. Metal.*, 25 (2015) 2898.
37. H.Z. Tavakoli, M. Abdollahy, S.J. Ahmadi, A.K. Darban, *Miner. Eng.*, 111 (2017) 36.
38. R. Yu, D. Zhong, L. Miao, F. Wu, G. Qiu, G. Gu, *T. Nonferr. Metal. Soc.* 21 (2011) 1634.
39. M. Lotfaliana, M. Ranjbarb, M.H. Fazaelipoorc, M. Schaffiec, Z. Manafid, *Miner. Eng.*, 81 (2015) 52.
40. N. Hiroyoshi, M. Tsunekawa, H. Okamoto, R. Nakayama, S. Kuroiwa, *Can. Metall. Q.*, 47 (2008) 253.
41. H. Kametani, A. Aoki, *Metall. Mater. Trans. B*, 16 (1985) 695.